Aquatic Mammals 2009, *35*(1), 36-42, DOI 10.1578/AM.35.1.2009.36

Normal Thoracic Radiographic Anatomy of Immature California Sea Lions (*Zalophus californianus*) and Immature Northern Elephant Seals (*Mirounga angustirostris*)

Sophie E. Dennison,[1] Lisa Forrest,[1] and Frances M. D. Gulland[2]

[1]*Department of Surgical Sciences (Radiology), School of Veterinary Medicine, 2015 Linden Drive, Madison, WI 53706, USA; E-mail: dennison@svm.vetmed.wisc.edu*
[2]*The Marine Mammal Center, 1065 Fort Cronkhite, Sausalito, CA 94965, USA*

Abstract

Immature California sea lions (*Zalophus californianus*) and northern elephant seals (*Mirounga angustirostris*) without evidence of thoracic disease were radiographed under anesthesia. Important species-specific variations were noted on thoracic radiographs. For the California sea lions, the mean vertebral heart score was 8.65 from the left lateral view, and the cardiac silhouette occupied a mean of 66% of the internal thoracic width. The tracheal bifurcation in California sea lions was located at the level of the first thoracic vertebral body. For the northern elephant seals, there was variation in the number of thoracic vertebrae and ribs from 12 to 15, a lack of pulmonary lobation, and an indistinct cardiac silhouette. Cardiac measurements could only be made on ventrodorsal (VD) and dorsoventral (DV) digital radiographs where the cardiac silhouette occupied a mean of 62% of the internal thoracic width. The combination of smooth to rounded lung lobe margins with border effacement of the cardiac silhouette and diaphragmatic margin is an important, normal, species-specific finding of the northern elephant seal that could be easily mistaken for pleural effusion. The carina in the northern elephant seals was at the level of the fifth thoracic vertebral body. In both species, the aortic bulb was evident as a focal, fairly symmetrical cranial mediastinal widening cranial to the cardiac silhouette on the VD and DV views, resulting in the aorta being identifiable on both the right and the left. This is an important normal finding in marine mammals that should not be mistaken for pathology. Both species had a diffuse bronchointerstitial pulmonary pattern that was slightly more prominent in California sea lions. This finding was consistent with variation between these species in the tissues supporting the small airways.

This prospective study serves as a normal reference for immature California sea lions and northern elephant seals in veterinary care.

Key Words: Radiology, radiography, diagnostic imaging, marine mammal, seal, vertebral heart score, lung, trachea, pinniped, California sea lion, *Zalophus californianus*, northern elephant seal, *Mirounga angustirostris*

Introduction

Pinnipeds are commonly maintained in public display facilities in the United States and require veterinary care to ensure their welfare under the Animal Welfare Act, first passed in 1966, administered by the U.S. Department of Agriculture (USDA) and implemented by the Animal and Plant Health Inspection Service (APHIS) (Young & Shapiro, 2001). Free-ranging individuals frequently strand and also require treatment before being returned to the free-ranging population (Colegrove et al., 2005; Greig et al., 2005). Two of the pinniped species that are examined frequently by veterinarians (Colegrove et al., 2005; Greig et al., 2005) are the California sea lion (*Zalophus californianus*), an otariid, and the northern elephant seal (*Mirounga angustirostris*), a phocid. Both species are members of the order Pinnipedia and have evolved for survival in an aquatic environment. Otariids and phocids have species-specific anatomical differences, however, that may affect radiographic evaluation of the thoracic cavity (Drabek, 1975; King, 1983). Knowledge of such species-specific variation is essential for the accurate differentiation between normalcy and pathology in order that an appropriate prescription of medical or surgical therapy can be made.

Pneumonia, whether parasitic or bacterial, is a common cause of morbidity and mortality in these species (Greig et al., 2005), and particularly it afflicts immature (pup and yearling) California sea lions (CSL). Furthermore, weaned northern elephant seal (NES) pups have frequently been diagnosed *post mortem* with *Otostrongylus circumlitus* infection of the pulmonary arteries and right ventricle of the heart (Gulland et al.,

1997; Colegrove et al., 2005) and megaesophagus due to a persistent right aortic arch (Maclean et al., 2008), both of which may initially be investigated in the live animal via thoracic radiographs. However, studies describing normal thoracic findings do not currently exist, making it difficult for the inexperienced interpreter to identify such abnormalities. Other than a book chapter (Van Bonn et al., 2001), the lack of normal thoracic findings in the literature hinders the publication of abnormal thoracic radiographic findings. The purpose of this prospective study was to describe normal thoracic radiographic anatomy in immature CSLs (weaned pups and yearlings) and immature NESs (weaned pups) and provide baseline data for future reference.

Materials and Methods

Weaned CSL pups, CSL yearlings, and weaned NES pups that were admitted to The Marine Mammal Center, Sausalito, California, without clinical evidence of pulmonary, cardiac, or pleural disease, with normal blood profiles (Bossart et al., 2001) and the absence of parasitic larvae in fecal samples were recruited for this study if an anesthetic was required for an unrelated reason. For CSLs, June 15 is the arbitrary date chosen as the start of the new pupping season, thus "pups" were those radiographed before June 15 and "yearlings" were those radiographed after June 15. Animals were anesthetized using a variety of protocols according to the individual's need and the attending veterinarian's preference (Haulena & Heath, 2001). Four-view radiographs of the thorax were taken of each animal: (1) ventrodorsal (VD), (2) dorsoventral (DV), (3) left lateral, and (4) right lateral. Careful positioning was required for radiographs to be considered of diagnostic quality. For the VD and DV views, this meant inclusion of both the thoracic inlet and caudal lung lobes, with at least partial superimposition of the sternum over the spine and abduction of the pectoral flippers away from the thoracic wall. For the lateral views, this meant inclusion of the cranial and caudal lung lobe margins, superimposition of the centrally located ribs, absence of superimposition of the proximal ribs over the spinous processes of the thoracic vertebrae, and ventral positioning of the pectoral flippers to minimize their superimposition. The x-ray beam was centered over the heart, the position of which was determined by observation of the apical heartbeat, and collimation was optimized.

Following positioning and before the radiographic exposure was made, the animal was permitted to take five deep breaths to reduce positional atelectasis. Sandbags, tape strips, and towels were used to maintain this position while personnel left the room during each exposure, and the exposure was timed to coincide with maximal inspiration. A combination of conventional film-screen and digital (direct) radiography was used. All radiographic images were reviewed by one author (SED) for the following: number of ribs; number of sternebrae; position of thoracic trachea and tracheal bifurcation (carina); and visibility of cardiac silhouette, cranial and caudal lobar vasculature, esophagus, and sternal, mediastinal, and tracheobronchial lymph nodes. Finally, cardiac silhouette size measurements were made, provided cardiac silhouette margins were distinct. For the VD and DV views, the percentage of the internal width of the thoracic cavity occupied by the cardiac silhouette was calculated by dividing the maximal right-to-left width of the cardiac silhouette by the internal thoracic cavity width (right-to-left measurement) at the same location (Figure 1). The vertebral heart score (VHS) was calculated after minor modification of Buchanan's method (Buchanan & Bucheler, 1995). The modification was necessary because of the cranial location of the tracheal bifurcation, which was unrelated to the cardiac base. The long-axis cardiac measurement was made from the ventral border of the ventral principle bronchus as the bronchi branch over the heart base to the cardiac apex (Figure 2). The short-axis cardiac measurement was made perpendicular to the long-axis measurement starting at the level of the dorsal margin of the caudal vena cava. The acquired values were then converted to vertebral lengths by measuring caudally from the cranial end plate of the fourth vertebral body on the lateral radiograph and summed to give the vertebral heart score (Buchanan & Bucheler, 1995; Lister & Buchanan, 2000).

Results

In total, 15 CSL pups and yearlings (eight male and seven female) and 10 NES pups (five male and five female) were examined. Causes for stranding in the recruited animals included malnutrition (nine CSLs and 10 NESs) and trauma affecting either the skull or flippers (six CSLs). A single radiographic image covered the entire thorax of all pinnipeds for all views. Radiographs with annotations identifying species-specific findings are shown in Figures 1 through 4. Specific numerical findings are tabulated in Table 1. Measurement data from male and female animals demonstrated complete overlap of values and thus were grouped together for analysis.

California Sea Lions (Figures 1 & 2)

No musculoskeletal abnormalities were identified on radiographs of any animal. The cardiac

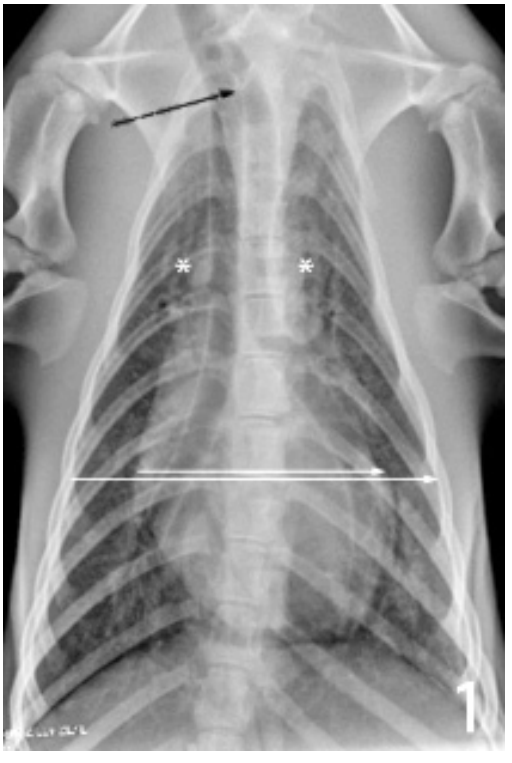

Figure 1. Dorsoventral radiographic view of a normal yearling California sea lion (*Zalophus californianus*) thorax; black arrow = carina (tracheal bifurcation) and * demonstrates the lateral margins of the aortic bulb. The cardiac silhouette is clearly identifiable. The white arrows demonstrate the measurements used to calculate the percentage of the thorax occupied by the cardiac silhouette. There is a normal, diffuse bronchointerstitial pattern throughout all lung fields. Right is to the left of the image.

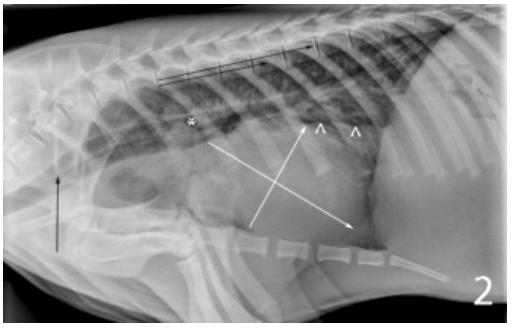

Figure 2. Left lateral radiographic view of a normal yearling California sea lion thorax; black arrow = carina, * = branching of principle bronchus, and ^ = dorsal margin of the caudal vena cava. White arrows demonstrate the modified measurements used to calculate the vertebral heart score (VHS). Note the long axis measurement is made from the ventral surface of the most ventral bronchus at the level of branching of the principle bronchus. The two measurements were converted to vertebral lengths by measuring caudally from the cranial end plate of the 4th thoracic vertebra, then summed to give the VHS. This conversion is shown by the two black arrows superimposed on the vertebral canal and, in this example, the VHS is 8.5. Note how well the cardiac silhouette is defined compared to the northern elephant seal example in Figure 4.

silhouette was identifiable in all animals in all views but had a shallower angle with the sternum than is seen in the domestic dog and cat. There was a focal, fairly symmetrical widening of the cranial mediastinum immediately cranial to the cardiac silhouette on the VD and DV views that corresponded to the aortic bulb of the ascending aorta. Right lateral cardiac measurements were consistently larger than the left lateral measurements for the same animal but were not significantly different ($p = 0.49$, $t = 0.73$, Student t test). The cardiac silhouette had a slightly rounder appearance on DV compared to VD views, but the percent of the internal width of the thorax occupied by the cardiac silhouette was not significantly different ($p = 0.09$, $t = 1.85$, Student t test). The caudal cardiac silhouette and ventral diaphragmatic margins were evident in all animals on all views.

The lung parenchyma had a diffuse interstitial to bronchointerstitial pattern. On VD and DV views, the trachea coursed sagittal or parasagittal (consistently right-sided) before branching at the level of the first thoracic vertebra. From there, the right and left principle bronchi continued caudally, located parasagittal on the VD and DV views and diverging slightly from the vertebral column on the lateral view toward the cardiac base. The esophagus was not identified on any view in any animal and neither were any soft tissue structures consistent with lymph nodes. The cranial mediastinum was parallel with the vertebral column between the thoracic inlet and aortic bulb on the VD and DV views and was only identified with some difficulty on the lateral views.

Northern Elephant Seals (Figures 3 & 4)

No musculoskeletal abnormalities were identified in any animal. Variations in the number of thoracic vertebrae from 12 to 15, and associated ribs, were observed: 7 of 10 NESs, had 15 thoracic vertebrae, 2 of 10 NESs had 13 thoracic vertebrae, and 1 of 10 NESs had 12 thoracic vertebrae. The cardiac silhouette was not definitively identifiable in any animal on the lateral view, thus the VHS calculations were not possible. The caudal cardiac silhouette and ventral diaphragm could not be distinguished on the lateral views due to border effacement. On the VD/DV views, the prominent aortic bulb was evident as a focal, fairly symmetrical widening of the cranial mediastinum

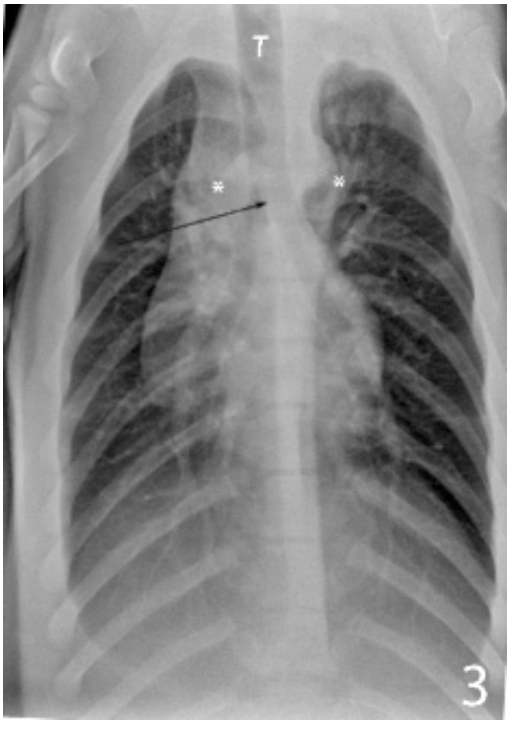

Figure 3. Dorsoventral radiographic view of a normal northern elephant seal (*Mirounga angustirostris*) thorax; T = trachea, black arrow = carina, and * = lateral margins of the aortic bulb. The cardiac silhouette is far more easily identified in this view compared to the lateral projection; however, border effacement remains evident between the caudal cardiac silhouette and the diaphragm. Note the rounded caudal margin of the lung lobes, which is normal for this species and not indicative of pleural effusion. Right is to the left of the image.

immediately cranial to the cardiac silhouette, and caused the aorta to be identifiable on both the right and left of midline. On the VD/DV views, the cardiac silhouette was identified in the three of ten animals that had radiographs taken using digital radiography.

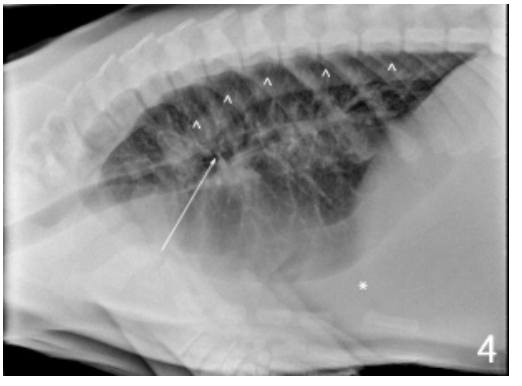

Figure 4. Left lateral radiographic view of a normal northern elephant seal thorax; white arrow = carina, white arrowheads = dorsal margin of the descending aorta, and * = border effacement between caudal cardiac silhouette and diaphragm. Note that the cardiac silhouette cannot be clearly defined on this view and that the ventral lung lobes are smooth without fissures. There is border effacement between the ventral diaphragmatic margin and the caudal cardiac silhouette, which is normal for this species and not indicative of pleural effusion. Note the diffuse interstitial pattern throughout all lung lobes.

The lung lobes did not fill the entire thorax and were poorly lobated as identified by the smooth ventral and caudal margins without fissures. A diffuse bronchointerstitial pattern throughout all lung lobes, similar to, but less remarkable than, the pattern identified in the CSL, was present. On VD and DV views, the trachea coursed sagittal or parasagittal (consistently right-sided) before branching at the level of the fifth thoracic vertebral body. From there, the bronchi continued caudally, either sagittal or parasagittal. The esophagus was not identified on any view in any animal and

Table 1. Observations from thoracic radiographs of California sea lion (*Zalophus californianus*) pups and yearlings and northern elephant seal (*Mirounga angustirostris*) pups; the cardiac silhouette could not be confidently identified from the lateral radiographic views in any northern elephant seal thus vertebral heart score measurements were not possible. CSL = California sea lion; NES = northern elephant seal; n/a = not applicable.

	CSL	NES
Modal number of ribs and thoracic vertebrae (range)	15 (n/a)	15 (12-15)
Number of sternebrae	8	8
Mean (95% CI) cardiac silhouette vertebral heart score:		
Right lateral (Rt lat)	8.75 (8.41-9.01)	Not
Left lateral (Le lat)	8.65 (8.39-8.90)	measurable
Mean width of cardiac silhouette to thoracic width as percentage:		
Ventrodorsal (VD)	63%	59%
Dorsoventral (DV)	66%	62%
Median (range) position of tracheal bifurcation compared to spine	T1 (C7-T1)	T5 (T4/5 to T5/6)

neither were any soft tissue structures consistent with lymph nodes.

Discussion

Herein, the normal thoracic radiographic anatomy in immature CSLs and NESs is described. Many differences exist when compared to domestic dogs and indeed each other; thus, it is imperative that veterinarians are familiar with the species-specific anatomy before attempting interpretation of such radiographic studies.

The increased pulmonary bronchointerstitial pattern present in the population reported herein is not surprising considering other reports have described increased connective tissue present for support of the airways (Green, 1972; King, 1983). One important anatomical difference between the CSL and the NES is the level at which cartilaginous support of the airways terminates. In the CSL, this termination is at the alveolar junction with the bronchioles, while in the NES, the termination is more proximal, within the small bronchi (Green, 1972; Simpson & Gardner, 1972; King, 1983). Furthermore, the distal small bronchioles of phocids are supported by muscle that bridges the gap between the termination of the cartilaginous support and the alveoli, a distance of approximately 2 mm. This lower airway development begins in the foetus but is not completed until several months of age (King, 1983). Cartilage and muscle will both attenuate x-rays more than the air-filled alveoli, resulting in an increase in radiographic opacity correlating with these regions. Additionally, respiratory tract cartilage has a tendency to mineralize, further increasing the attenuation properties of the tissue and further increasing the resultant radiographic opacity (Berry et al., 2007). This infers that a mild, diffuse, and uniform bronchointerstitial pattern is a normal finding in both species and should be slightly more pronounced in the CSL due to the greater amount of cartilagenous support that may mineralize. The difference in pulmonary pattern identified between the animals studied herein may also, in part, represent the slight age difference. NES weaned pups, approximately 3 to 6 mo of age, would likely have still been developing the support surrounding the airways (King, 1983), whereas the ages of the weaned CSL pups and yearlings, estimated to have ranged from approximately 9 to 15 mo, suggest that lower airway support would have been fully developed. The animals recruited for this study were from the age groups for each species commonly admitted into rehabilitation, and this normal difference in pulmonary pattern between the species is important to recognize.

A general reduction in lung lobation has been identified in all phocid species compared to otariid species, with almost negligible lobation evident in some. This variation is thought to correlate with differing diving behaviours (King, 1983). The reduced lung lobation of phocids was demonstrated radiographically in the NES by rounded caudal and ventral lung margins, a lack of fissure lines, and border effacement between the caudal cardiac silhouette and the diaphragm. This combination of border effacement with rounded lung lobe margins in the NES could be mistaken for an abnormality such as pleural effusion (Lord et al., 1972). Hence, this is an extremely important species-specific variation to note during interpretation of thoracic radiographs. Conversely, the lung lobation in the CSL is similar to terrestrial mammals (King, 1983) and, as a result, the CSL thoracic radiograph more closely resembled the radiograph of the dog than the radiograph of the NES. Thus, evidence of border effacement and rounded lung lobe margins in CSL radiographs should be considered clinically significant as it is in the dog (Lord et al., 1972).

The pulmonary lobar vasculature was difficult to define due to the background pulmonary pattern. The caudal lobar vasculature was the easiest to evaluate and was best defined on the DV view as previously described in other species (Kirberger & Avner, 2006). This was similar for both species.

In the CSL, the carina was identified at the level of the first thoracic vertebra, markedly cranial to the level of the heart base where the carina is located in dogs and cats (Berry et al., 2007) and consistent with previous reports (King, 1983). It is interesting to note that the NES carina was positioned at the level of the fifth thoracic vertebra, near the site where the principle bronchi insert into the parenchyma of the lung (King, 1983). This variation in carina position has clinical implications particularly for endotracheal intubation (Haulena & Heath, 2001).

The pinniped heart has the same anatomy as dogs and cats but is flatter and broader in shape (King, 1983). In this study, the cardiac silhouette occupied approximately 63 to 66% of the thorax in CSLs and 52 to 62% in NESs, and this small difference between species was most likely due to their different body conformations as accounts for similar variations in different breeds of dogs (Berry et al., 2007), with CSLs more deep-chested and NESs being more barrel-chested. Similar to previous studies in dogs, the cardiac silhouette was slightly elongated on VD views compared to DV views (Kirberger & Avner, 2006). Buchanan's vertebral heart score has been used in dogs (Buchanan & Bucheler, 1995) and in cats (Lister & Buchanan, 2000) to determine cardiomegaly vs normalcy. In those species, the long-axis measurement was made through the

heart from the carina to the cardiac apex. While the CSL carina was not positioned over the heart base, the branching of the principle bronchus into secondary bronchi was repeatedly evident over the heart base. This observation led to modification of Buchanan's method by the authors, using the branching of the principle bronchus over the heart base as the landmark for the long axis measurement. The long and short axis measurements were then converted into vertebral lengths and summed to give a VHS as performed in dogs and cats. Using this method, cardiac size in the CSL was determined to have a mean and 95% CI of 8.6 and 8.39 to 8.9 vertebral lengths, respectively, from the left lateral view. Thus, the cardiac size in CSLs measured smaller than the VHS of 9.7 +/- 0.5 described in dogs by Buchanan & Bucheler (1995) and larger than the 7.5 +/- 0.3 described in cats by Lister & Buchanan (2000). The cardiac size was smaller on the left lateral view than the right lateral view in 13 of 15 CSLs as expected from positional radiographic studies (Kirberger & Avner, 2006; Greco et al., 2008). Interestingly, two of 15 CSLs did not follow this trend, instead demonstrating larger VHS from their left lateral radiographs. This can be explained by considering the bradycardia that occurs during an anesthesia-induced dive reflex (Kooyman et al., 1981; King, 1983; Haulena & Heath, 2001), resulting in a comparatively longer duration of systole. This was not specifically studied herein, however.

Mature CSLs and NESs demonstrate sexual dimorphism (Green, 1972; King, 1983). The cardiac measurement data acquired for males and females for both species described herein demonstrated complete overlap, and thus the data were grouped together. As immature animals were used for this study, a lack of differentiation between male and female data is not surprising. Potential variation in normal cardiac size ranges between mature male and female animals should not be ignored, and more work is needed to determine this. However adult NESs are rarely found in captivity and are unlikely to be admitted into the rehabilitation setting (Gulland, pers. comm.).

The cranial mediastinum was focally and fairly symmetrically widened in both species immediately cranial to the cardiac silhouette on the VD/DV view. The widening was most easily identified on these views but could also be seen on the lateral views with careful evaluation, and it corresponded with the location of the aortic bulb. The aortic bulb of marine mammal species is an elastic enlargement of the ascending aorta that varies in comparative size according to species (Drabek, 1975; King, 1983; Ponganis, 2002). The enlargement is maximal through the region where the brachiocephalic trunk and carotid and subclavian arteries originate (King, 1983). The ascending aorta diameter gradually increases from its origin to its maximal dimension at the aortic bulb and then suddenly decreases in diameter at the level of the ductus arteriosus or ligamentum arteriosus. From here, the descending aorta is uniform in diameter and approximately 50% of the diameter of the aortic bulb (King, 1983). On VD and DV radiographs, the aortic bulb permits identification of the aorta on the right before it crosses midline to assume the familiar left-sided position identified in dogs and cats (Berry et al., 2007). The aortic bulb is an adaptation for diving and is believed to maintain blood pressure and thus cardiac and brain perfusion during the prolonged diastole associated with dive-induced bradycardia (Drabek, 1975; Ponganis, 2002). It is an extremely important variation found in marine mammals and should not be mistaken for pathology.

Variation in skeletal, and more specifically, vertebral morphology has been described before in marine and terrestrial mammals alike (Green, 1972; Ferrell et al., 2007; Newitt et al., 2008). The number of ribs will vary with the number of thoracic vertebrae. While 15 thoracic vertebrae and rib pairs were identified in all CSLs, the number of thoracic vertebrae and rib pairs was less than 15 in 3 of the 10 NESs. Congenital abnormalities are known to occur frequently in NESs, affecting around 5% of stranded pups (Trupkiewicz et al., 1997). Bonnell & Selander (1974) proposed that the frequency with which they are seen relates to the recovery of the NES population from devastatingly low numbers and a subsequent restricted gene pool. The congenital skeletal variations such as described herein are unlikely to be of clinical significance (Ferrell et al., 2007; Newitt et al., 2008). The actual frequency with which they occur within the general population is not known and was not specifically investigated as part of this study.

One limitation in this study is the presumptive, rather than proven, normalcy of the thoraces that were radiographed. All animals included in the study were successfully rehabilitated and released, thus necropsy data were not available to correlate with radiographic findings. However, the absence of clinical signs associated with pulmonary or cardiac pathology, normal blood profiles, and fecal samples devoid of parasitic larvae plus subsequent release into the free-ranging population without restranding is strongly suggestive of normalcy. In addition, all findings were uniform and consistent among animals examined as part of this study. Thus, we propose the results of this study as normal thoracic radiographic anatomy for immature CSLs and NESs.

Acknowledgments

This study was approved by The Marine Mammal Center, Sausalito, California, Institutional Animal Care and Use Committee (IACUC). The authors would like to thank Dr. Felicia Nutter, DVM, Michelle Blascow, RVT, Amber Makie, RVT, and Deb Wickham, RVT, Department of Veterinary Science, The Marine Mammal Center for assistance in selection of suitable recruits and acquisition of radiographic images.

Literature Cited

Berry, C. R., Graham, P. R., & Thrall, D. E. (2007). Interpretation paradigms for the small animal thorax. In D. E. Thrall (Ed.), *Textbook of veterinary diagnostic imaging* (5th ed.) (pp. 462-485). St. Louis: Saunders-Elsevier.

Bonnell, M. L., & Selander, R. K. (1974). Elephant seals: Genetic variation and near extinction. *Science*, *184*, 908-909.

Bossart, G. D., Reidarson, T. H., Dierauf, L. A., & Duffield D. A. (2001). Clinical pathology. In L. A. Dierauf & F. M. D. Gulland (Eds.), *CRC handbook of marine mammal medicine* (2nd ed.) (pp. 383-430). Boca Raton, FL: CRC Press.

Buchanan, J. W., & Bucheler, J. (1995). Vertebral scale system to measure canine heart size in radiographs. *Journal of the American Veterinary Medical Association*, *206*, 194-199.

Colegrove, K. M., Greig, D. J., & Gulland, F. M. D. (2005). Causes of live strandings of northern elephant seals (*Mirounga angustirostris*) and Pacific harbor seals (*Phoca vitulina*) along the central California coast, 1992-2001. *Aquatic Mammals*, *31*(1), 1-10.

Drabek, C. M. (1975). Some anatomical aspects of the cardiovascular system of Antarctic seals and their possible functional significance in diving. *Journal of Morphology*, *145*, 85-106.

Ferrell, E. A., Berry, C. R., & Thrall, D. E. (2007). Technical issues and interpretation principles relating to the axial skeleton. In D. E. Thrall (Ed.), *Textbook of veterinary diagnostic imaging* (5th ed.) (pp. 94-105). St. Louis: Saunders-Elsevier.

Greco, A., Meomartino, L., Raiano, V., Fatone, G., & Bonnetti, A. (2008). Effect of left versus right recumbency on the vertebral heart score in normal dogs. *Veterinary Radiology and Ultrasound*, *49*(5), 454-455.

Green, R. F. (1972). Observations of anatomy of some cetaceans and pinnipeds. In S. H. Ridgway (Ed.), *Mammals of the sea* (pp. 271-293). Springfield, IL: Charles C. Thomas.

Greig, D. J., Gulland, F. M. D., & Kreuder, C. (2005). A decade of live California sea lion (*Zalophus californianus*) strandings along the central California coast: Causes and trends, 1991-2000. *Aquatic Mammals*, *31*(1), 11-22.

Gulland, F. M. D., Beckman, K., Burek, K., Lowenstine, L. J., Werner, L., Spraker, T., et al. (1997). Nematode (*Otostrongylus circumlitus*) infestation of northern elephant seals (*Mirounga angustirostris*) stranded along the central California coast. *Marine Mammal Science*, *13*(3), 446-459.

Haulena, M., & Heath, R. B. (2001). Marine mammal anesthesia. In L. A. Dierauf & F. M. D. Gulland (Eds.), *CRC handbook of marine mammal medicine* (2nd ed.) (pp. 655-684). Boca Raton, FL: CRC Press.

King, K. E. (1983). *Seals of the world*. Ithaca, NY: Cornell University Press.

Kirberger, R. M., & Avner, A. (2006). The effect of positioning on the appearance of selected cranial thoracic structures in dogs. *Veterinary Radiology and Ultrasound*, *41*(1), 61-68.

Kooyman, G. L., Castellini, M. A., & Davis, R. W. (1981). Physiology of diving in marine mammals. *Annual Review of Physiology*, *43*, 343-356.

Lister, A. L., & Buchanan, J. W. (2000). Vertebral scale system to measure heart size in radiographs of cats. *Journal of the American Medical Association*, *216*, 210-214.

Lord, P. F., Suter, P. F., Chan, K. F., Appleford, M., & Root, C. R. (1972). Pleural, extrapleural and pulmonary lesions in small animals: A radiographic approach to differential diagnosis. *Journal of the American Radiologic Society*, *13*, 4-17.

Maclean, R. A., Imai, D., Dold, C., Haulena, M., & Gulland, F. M. D. (2008). Persistent right aortic arch and cribriform plate aplasia in a northern elephant seal (*Mirounga angustirostris*). *Journal of Wildlife Diseases*, *44*(2), 499-504.

Newitt, A., German, A. J., & Barr, F. J. (2008). Congenital abnormalities of the feline vertebral column. *Veterinary Radiology and Ultrasound*, *49*(1), 35-41.

Ponganis, P. J. (2002). Circulatory system. In W. F. Perrin, B. Würsig, & J. G. M. Thewissen (Eds.), *Encyclopedia of marine mammals* (pp. 229-234). San Diego: Academic Press.

Simpson, J. G., & Gardner, M. B. (1972). Comparative microscopic anatomy of selected marine mammals. In S. H. Ridgway (Ed.), *Mammals of the sea* (pp. 299-333). Springfield, IL: Charles C. Thomas.

Trupkiewicz, J. G., Gulland, F. M. D., & Lowenstine, L. J. (1997). Congenital defects in northern elephant seals stranded along the central California coast. *Journal of Wildlife Diseases*, *33*(2), 220-225.

Van Bonn, W., Jensen, E. D., & Brook, F. (2001). Radiology, computed tomography and magnetic resonance imaging. In L. A. Dierauf & F. M. D. Gulland (Eds.), *CRC handbook of marine mammal medicine* (2nd ed.) (pp. 557-590). Boca Raton, FL: CRC Press.

Young, N. M., & Shapiro, S. L. (2001). U.S. federal legislation governing marine mammals. In L. A. Dierauf & F. M. D. Gulland (Eds.), *CRC handbook of marine mammal medicine* (2nd ed.) (pp. 741-766). Boca Raton, FL: CRC Press.